

Taxol Suppresses Dynamics of Individual Microtubules in Living Human Tumor Cells

Anne-Marie C. Yvon,* Patricia Wadsworth,* and Mary Ann Jordan^{†‡}

*Molecular and Cellular Biology Program, University of Massachusetts, Amherst, Massachusetts, 01003; and [†]Department of Molecular, Cellular, and Developmental Biology, University of California, Santa Barbara, California, 93106

Submitted September 3, 1998; Accepted January 19, 1999
Monitoring Editor: Marc W. Kirschner

Microtubules are intrinsically dynamic polymers, and their dynamics play a crucial role in mitotic spindle assembly, the mitotic checkpoint, and chromosome movement. We hypothesized that, in *living* cells, suppression of microtubule dynamics is responsible for the ability of taxol to inhibit mitotic progression and cell proliferation. Using quantitative fluorescence video microscopy, we examined the effects of taxol (30–100 nM) on the dynamics of individual microtubules in two living human tumor cell lines: Caov-3 ovarian adenocarcinoma cells and A-498 kidney carcinoma cells. Taxol accumulated more in Caov-3 cells than in A-498 cells. At equivalent intracellular taxol concentrations, dynamic instability was inhibited similarly in the two cell lines. Microtubule shortening rates were inhibited in Caov-3 cells and in A-498 cells by 32 and 26%, growing rates were inhibited by 24 and 18%, and dynamicity was inhibited by 31 and 63%, respectively. All mitotic spindles were abnormal, and many interphase cells became multinucleate (Caov-3, 30%; A-498, 58%). Taxol blocked cell cycle progress at the metaphase/anaphase transition and inhibited cell proliferation. The results indicate that suppression of microtubule dynamics by taxol deleteriously affects the ability of cancer cells to properly assemble a mitotic spindle, pass the metaphase/anaphase checkpoint, and produce progeny.

INTRODUCTION

Microtubules are intrinsically dynamic polymers, undergoing two kinds of dynamic behavior: dynamic instability and treadmilling. In dynamic instability, microtubule ends stochastically switch between episodes of prolonged growing and shortening (Mitchison and Kirschner, 1984). One microtubule end, the plus end, shows more dynamic behavior than the opposite end, the minus end. The other form of dynamic behavior, treadmilling, consists of net growing at microtubule plus ends and net shortening at minus ends (Margolis and Wilson, 1978; Rodionov and Borisy, 1997). Microtubule dynamics are important to many functions in cells, the most dramatic of which is mitosis. When cells enter mitosis, the interphase cytoskeletal microtubule array is disassembled and a bipolar spindle is assembled. Spindle microtubules

attach to chromosomes at the kinetochore and contribute to chromosome alignment and subsequent segregation at anaphase. Microtubule dynamics are relatively slow in interphase cells, but increase 10- to 100-fold at mitosis (Saxton *et al.*, 1984; Pepperkok *et al.*, 1990; Zhai *et al.*, 1996). Both extensive dynamic instability and treadmilling occur in mitotic spindles, and the rapid dynamics of spindle microtubules play a critical role in the intricate movements of the chromosomes (Mitchison, 1989; Hayden *et al.*, 1990; Rieder *et al.*, 1994; Waterman-Storer and Salmon, 1997). In addition, evidence is accumulating that microtubule dynamics may play a crucial role in passage through the metaphase/anaphase checkpoint (Jordan *et al.*, 1992, 1993; Dhamodharan *et al.*, 1995; McEwen *et al.*, 1997; Sorger *et al.*, 1997; Vasquez *et al.*, 1997; Jordan and Wilson, 1998a,b).

Taxol is an important new cancer chemotherapeutic agent that is effective in the treatment of many types of

[‡] Corresponding author. E-mail address: jordan@lifesci.lscf.ucsb.edu.

cancer, including carcinoma of the ovary, lung, head and neck, bladder, and esophagus (Rowinsky, 1997). The principal chemotherapeutic target of taxol is microtubules (Schiff *et al.*, 1980; Horwitz, 1992). The action of taxol on microtubules in cells has generated much excitement because the drug's antitumor potency has been hypothesized to be linked to a unique mechanism of action. Although most antimetabolic drugs (e.g., vinblastine, estramustine, dolastatins, and cryptophycin) depolymerize microtubules in cells at relatively high drug concentrations, high concentrations of taxol (>100 nM) greatly increase microtubule polymer mass in cells and induce the formation of extensive bundles of microtubules (Schiff and Horwitz, 1980; Jordan *et al.*, 1992, 1993), which may be involved in the ability of taxol to inhibit cell proliferation (Rowinsky *et al.*, 1988); however, we discovered that even at low concentrations that do not significantly increase microtubule polymer levels or induce microtubule bundling, taxol strongly inhibits HeLa cell proliferation (Jordan *et al.*, 1993). These data suggested that it may be the suppression of microtubule dynamics, rather than the stimulation of microtubule polymerization and stabilization, that is the most sensitive and potent antitumor mechanism of taxol in cells. Interestingly, suppression of microtubule dynamics is the most potent mechanism of action of vinblastine and perhaps of several other anticancer drugs, suggesting that suppression of dynamics is the common mechanism for antimetabolic drugs (Wilson and Jordan, 1995; Jordan and Wilson, 1998; Panda *et al.*, 1998).

Taxol binds reversibly to microtubules with high affinity and with a maximum stoichiometry of 1 mol of taxol/mol of tubulin in microtubules (Parness and Horwitz, 1981; Diaz and Andreu, 1993; Caplow *et al.*, 1994). High concentrations of taxol enhance microtubule polymerization and stabilize microtubules to depolymerization by cold temperature, calcium ions, dilution, and other antimetabolic drugs such as vinblastine (Schiff *et al.*, 1979; Kumar, 1981; Howard and Timasheff, 1988). Importantly, the binding of only a few molecules of taxol to microtubules reassembled from purified bovine brain tubulin has recently been found to suppress microtubule dynamic instability, preferentially at microtubule plus ends (Jordan *et al.*, 1993; Derry *et al.*, 1995, 1998). For example, at 50 nM taxol, the microtubule shortening rate is suppressed by 32%, with a stoichiometry of one taxol molecule bound per 151 tubulin dimers in the microtubules. Suppression of dynamic instability is accompanied by only a modest increase in the polymer mass of reassembled bovine brain microtubules.

We have hypothesized that, in cells, suppression of microtubule dynamics is responsible for the potent ability of taxol to inhibit mitotic progression and cell proliferation. The manner in which taxol affects the

dynamic instability of individual microtubules in living cells has not been demonstrated, and we do not yet know whether its mode of action resembles that observed *in vitro*. In cells, taxol potently blocks or slows mitosis at the transition from metaphase to anaphase (Jordan *et al.*, 1993; Rieder *et al.*, 1994). Inhibition of progress through mitosis ultimately results in apoptotic cell death and may be important in the antitumor actions of the drug (Milas *et al.*, 1995; Jordan *et al.*, 1996).

In this work, we have examined the action of taxol on individual microtubule dynamics in living interphase human ovarian and kidney tumor cells. We found that taxol, at equivalent intracellular concentrations, suppressed the rates of growing and shortening of individual microtubules in both types of tumor cells. The concentration of taxol that suppressed dynamics in interphase cells was also found to inhibit cell proliferation and block mitosis by preventing progression from metaphase to anaphase. Together these observations strongly indicate that the mechanism of inhibition of mitosis by taxol is due to inhibition of microtubule dynamics.

MATERIALS AND METHODS

Materials

All materials for cell culture were obtained from Life Technologies-BRL (Gaithersburg, MD), with the exception of fetal calf serum, which was obtained from Hyclone Laboratories (Logan, UT). Unless otherwise noted, all other chemicals were obtained from Sigma (St. Louis, MO). Taxol (Molecular Probes, Eugene, OR) was prepared as a stock concentration of 10 mM in methanol, and aliquots were kept at -20°C . Intermediate dilutions were made in buffer (0.1 M PIPES, pH 6.9, 2 mM EGTA, 1 mM MgSO_4) before diluting to the final concentration in cell culture media.

Cell Culture and Proliferation

A-498¹ epithelial-like human kidney carcinoma cells (ATCC HTB 44) were grown in 90% MEM, supplemented with 1.0 mM sodium pyruvate; Caov-3 epithelial-like human ovarian adenocarcinoma cells (ATCC HTB 75) were grown in 90% DMEM, supplemented with 4.5 g/l glucose. Both cell lines were grown in 10% fetal calf serum and antibiotics, with 5% CO_2 , at 37°C . Doubling times were 32.9 ± 2.0 h for Caov-3 and 26.1 ± 1.7 h for A-498 cells. To determine the effects of taxol on cell proliferation, cells were seeded at $3\text{--}5 \times 10^4$ cells/ml, and 2 d later the medium was replaced with medium containing taxol. Cells were counted with a hemocytometer at the time of taxol addition and 24 h later.

Determination of the Intracellular Taxol Concentration

Cells were seeded directly into polylysine-coated scintillation vials (Research Products International, Mount Prospect, IL) at a density of 1.5×10^4 cells/ml (2.5 ml/vial). After 1 d of incubation (37°C) to

¹ Abbreviations used: A-498, human kidney carcinoma; Caov-3, human ovarian adenocarcinoma; PBS, 136 mM NaCl, 2.68 mM KCl, 1.47 mM KH_2PO_4 , 4.29 mM $\text{Na}_2\text{HPO}_4 \cdot 7\text{H}_2\text{O}$, pH 7.3; PBS-Tw-Az, PBS containing 0.1% Tween 20 and 0.02% azide.

allow cells to adhere to the glass, the media was replaced with fresh media containing [^3H]taxol (a kind gift of R. D. Haugwitz, National Cancer Institute, and provided by Research Triangle Institute, NSC#125973) (3 nM-1 μM ; specific activity 0.025–8 Ci/mol). The taxol-containing media was removed 4–24 h later, and the cells were rapidly washed and lysed (Jordan *et al.*, 1998) in distilled water and scintillation fluid (Ready Protein +, Beckman Instruments, Fullerton, CA), and radioactivity was determined. Total cell volume was determined by multiplying the cell number by the mean cell volume, determined from measurements of the diameter of 30 cells of each line after rounding of cells in trypsin; the mean volume of Caov-3 cells was 5.25 pl/cell and of A-498 cells was 6.8 pl/cell. Three independent experiments were performed for each taxol concentration and duration of uptake. Radioactivity was determined from duplicate vials, and adherent cells were determined in two to four vials for each condition.

Microinjection

Cells were plated on etched glass coverslips (Bellco Glass, Vineland, NJ) 24–72 h before use. For microinjection and subsequent observation, cells were transferred to media containing 10 mM HEPES buffer, lacking bicarbonate. Pressure microinjection was performed on a Zeiss IM-35 inverted microscope using a 32 \times phase objective lens, an Eppendorf 5242 microinjector, and a Narishige micromanipulator. Needles were pulled from Omega Dot capillary glass tubes (Friedrich & Dimmock, Millville, NJ) on a Brown-Flaming P-80 Micropipette Puller (Sutter Instruments, San Rafael, CA). Rhodamine-labeled porcine tubulin, prepared as described previously (Shelden *et al.*, 1993), was microinjected at a concentration of 2.2 mg/ml. Solutions to be microinjected were centrifuged in an Eppendorf 5415C centrifuge (Eppendorf, Madison, WI) at 14,000 rpm for 15 min immediately before injection, and the supernatant was transferred to a clean tube. After injection, the cells were returned to a 37°C incubator for at least 90 min to allow incorporation of the labeled tubulin into microtubules.

Low Light Level Microscopy and Image Acquisition

Microinjected cells were placed in a Rose chamber (Rose *et al.*, 1958) and observed using a Zeiss IM35 inverted microscope (Carl Zeiss, Thornwood, NY) maintained at $36 \pm 1^\circ\text{C}$ by an air curtain incubator. Images of rhodamine-labeled microtubules in the injected cells were obtained as described previously, using a 100 \times 1.3 numerical aperture Nikon apochromat lens (Shelden and Wadsworth, 1993). A Dage ISIT video camera (Wabash, MI), operated at maximum gain, was used to collect images, which were digitized using a Perceptics Pixel Pipeline card in a Macintosh Quadra 950 running BDS Image software (Oncor Inc, Gaithersburg, MD). Thirty-two-frame averages were collected at 2-s intervals, stored on a Perceptics Pixel Buffer store card, and subsequently transferred to optical discs.

Analysis of Microtubule Dynamics

Quantification of microtubule dynamic behavior was performed using laboratory-written software (Shelden and Wadsworth, 1993). The position of the plus end of an individual microtubule in a sequence of images was marked using a mouse-driven cursor; the position information was used to create a microtubule "life history" plot using the Cricket Graph program (Cricket Software, Malvern, PA). Phases of growth, shortening, and pause were marked on the plots; additional in-house software was used to determine the duration, distance, and rate of growth and shortening events and the duration of pause events. Only changes of $>0.5 \mu\text{m}$ were considered growth or shortening events. Data for each microtubule were entered into a spreadsheet (Kaleidagraph, Synergy Software, Reading, PA) for statistical analysis. The frequency of catastrophe was determined by dividing the sum of the number of transitions from growth to shortening and pause to shortening by either the sum of

the distance grown or the sum of the time in growth and pause. The frequency of rescue was determined by dividing the sum of the number of transitions from shortening to growth and from shortening to pause by the time spent shortening or the distance shortened. Dynamicity was calculated by dividing the sum of the total length grown and shortened by the life-span of the particular microtubule. The minus ends of microtubules were relatively nondynamic, as reported in Yvon and Wadsworth (1997); thus we did not measure the effects of taxol on minus ends.

Immunofluorescence Microscopy

Immunofluorescence localization of microtubules was performed on cells that were fixed in methanol for 10 min. Cells were rinsed in PBS containing 0.1% Tween 20 and 0.02% azide (PBS-Tw-Az) and then incubated for 1 h at 37°C in a monoclonal anti- α -tubulin antibody (DM1a; 1:100 dilution in PBS-Tw-Az with 1% bovine serum albumin). Cells were then rinsed in PBS-TW-Az and incubated with affinity-purified, fluorescein-conjugated, goat anti-mouse secondary antibodies (Organon Teknika, Durham, NC; 1:50 dilution in PBS-Tw-Az with 1% bovine serum albumin) for 30–45 min (25°C). In cases where chromosomes were to be examined, coverslips were subsequently stained with propidium iodide (Molecular Probes; 1:300 dilution in PBS-Tw-Az of 150 μM solution) for 5 min at room temperature. Stained cells were mounted in 90% glycerol containing 0.1% *p*-phenylenediamine and sealed with nail polish. Confocal microscopy of immunofluorescence preparations was performed using an argon ion laser scanning head (model MRC-600, Bio-Rad, Cambridge, MA) mounted on a Nikon Diaphot 200, equipped with a 60 \times 1.4 numerical aperture objective lens. Images were collected with the pinhole approximately one-third open. Images of interphase cells are 6 Kalman averages of the same plane in the z-axis; images of mitotic cells are an extended focus series, with 6 Kalman averages each of 10 1- μm optical sections. Images were opened using Adobe Photoshop software running on a Macintosh 8100 and printed for reproduction using a Tektronix Phaser 440 printer.

Mitotic index, mitotic spindle organization, and interphase morphology were determined on cells that were fixed in 10% formalin in PBS (25°C) followed by post-fixation in methanol (4°C). Microtubules were visualized with a mouse monoclonal antibody (E7, IG1; a gift from Dr. Michael Klymkowsky, University of Colorado, Boulder, CO) and fluorescein-conjugated goat anti-mouse IgG. Chromosomes were stained with DAPI.

Cell death was determined by staining unfixed cells with ethidium homodimer, which stains dead cells, and with calcein-AM, which is enzymatically cleaved by and stains live cells (Molecular Probes).

RESULTS

Recent experiments have shown that taxol blocks dynamic instability of microtubules reassembled *in vitro* (Jordan *et al.*, 1993; Derry *et al.*, 1995, 1998). This observation led to the hypothesis that taxol's ability to block mitosis and cell proliferation results from its suppression of dynamic instability *in vivo* (Jordan *et al.*, 1993, 1996; Wilson and Jordan, 1995; Jordan and Wilson, 1998). The goal of the present experiments was to directly measure taxol's effects on microtubule dynamic instability in living cells. In addition, it has been shown that taxol displays different potencies against tumors of various origins (Rowinsky and Donehower, 1995); the mechanism responsible for this effect is not known. To address this issue, we measured microtubule behavior in two diverse human

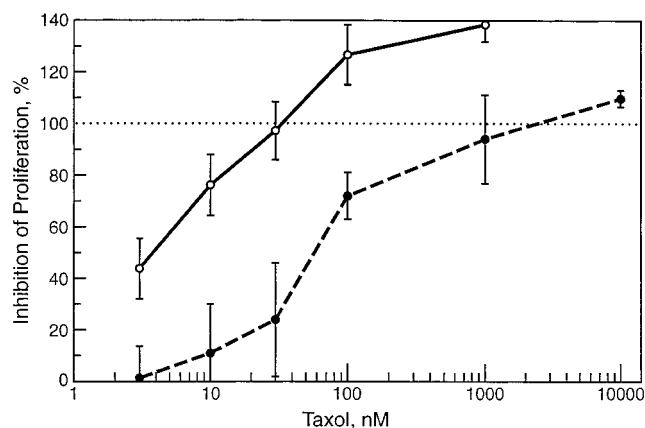


Figure 1. Inhibition of proliferation of Caov-3 ovarian carcinoma cells (○) and A-498 kidney carcinoma cells (●) by taxol (24 h). Cell proliferation was determined by counting live cells at the time of taxol addition and 24 h later. Values >100% inhibition of proliferation indicate net loss of cells over the 24-h duration of taxol incubation. Values are means and SEs of 11 independent experiments for A-498 cells and 4 experiments for Caov-3 cells.

tumor cell types, Caov-3 ovarian adenocarcinoma cells and A-498 kidney carcinoma cells, to determine whether taxol's effects on dynamic instability were cell-type specific.

Low Concentrations of Taxol Inhibit Proliferation in Caov-3 Ovarian Adenocarcinoma Cells and A-498 Kidney Carcinoma Cells

The goal of these experiments was to measure microtubule dynamics in living cancer cells at the lowest taxol concentrations that significantly inhibited proliferation. To measure effects of taxol on cell proliferation, cells were incubated with a range of taxol concentrations, and the increase in live cell number over 24 h was determined and compared with the increase in live cell number in a parallel culture in the absence of taxol. The taxol concentration dependence of inhibition of cell proliferation is shown in Figure 1; 30 nM taxol (24 h) completely inhibited proliferation of Caov-3 cells, and concentrations >30 nM induced some net loss of cell number, presumably a result of cell killing. Higher concentrations of taxol were required to significantly inhibit proliferation of A-498 kidney cells; incubation with 100 nM taxol (24 h) inhibited proliferation by 72.1% (Figure 1), and incubation for longer durations (48–72 h) completely inhibited proliferation (our unpublished results).

Different Accumulation of Taxol in Human Tumor Cells

The uptake of [³H]taxol (3–1000 nM) into Caov-3 and A-498 cells was measured (Table 1). Caov-3 cells incubated with 3 nM [³H]taxol for 24 h accumulated taxol

Table 1. Intracellular taxol concentration in human tumor cells after incubation for 24 h (or 4 h where noted) in taxol-containing medium and effects on proliferation

Cell type	Initial taxol concentration in media (nM)	Intracellular taxol concentration (μM)	Degree of concentration
Caov-3 ovarian carcinoma cells	3	3.6 ± 0.8	1200×
	10	13.5 ± 0.8	1350×
	30 (4 h)	10.7 ± 0.7	
	100	47.7 ± 2.2	477×
	1000	99.7 ± 20.6	100×
A-498 kidney carcinoma cells	3	1.0 ± 0.1	330×
	10	2.8 ± 0.3	280×
	100 (4 h)	19.6 ± 2.6	
	100	17.4 ± 1.8	174×
	1000	67.3 ± 3.6	67×

Values are mean ± SEM.

1200-fold intracellularly, to a concentration of 3.6 ± 0.8 μM. At higher taxol concentrations, the internal concentration increased to very high levels. For example, at 100 nM added taxol, the internal concentration in Caov-3 cells was 47.7 ± 2.2 μM. Taxol accumulated to a lesser extent in A-498 cells. At 3 nM added taxol, the internal concentration increased 330-fold to 1.0 ± 0.1 μM, and at 100 nM added taxol the internal concentration was 17.4 ± 1.8 μM at 24 h. Thus, taxol accumulated to a greater extent in Caov-3 cells than A-498 cells at all concentrations examined. The greater accumulation of taxol in ovarian cells may contribute to the more potent effect of taxol on ovarian cancer.

Microtubule Dynamics in Untreated Caov-3 Ovarian Tumor Cells and A-498 Kidney Tumor Cells

To compare the effects of taxol on microtubule dynamic instability in these two cell lines, it was important to use equivalent intracellular taxol concentrations. Extrapolation from the 24-h taxol uptake results reported above suggested that equivalent (10–20 μM) taxol concentrations would be attained by 4-h incubation of Caov-3 cells with ~30 nM taxol and of A-498 cells with 100 nM taxol. Also, these concentrations induced significant inhibition of proliferation in 24 h of incubation (100% in Caov-3 cells and 72.1% in A-498 cells). The time courses of taxol uptake into cells and of equilibration of fluorescent tubulin with microtubules in cells required careful timing of the microinjections and the drug incubation. In addition, optimum conditions for studying microtubule dynamics in living cells require that measurements be taken within a few hours after microinjection of fluorescent tubulin. Because taxol is known to stabilize microtubules, and could potentially reduce incorporation of

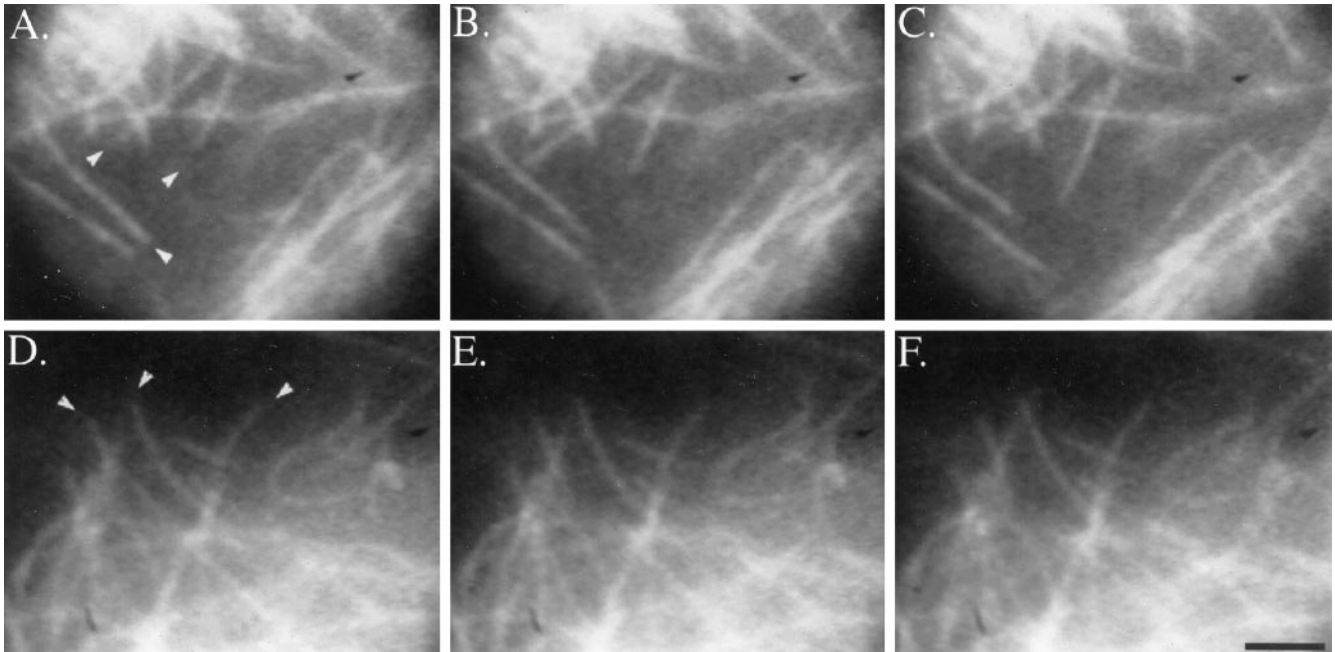


Figure 2. Dynamic behavior of microtubules in living Caov-3 cells in the absence of drug (A–C) or incubated with 30 nM taxol for 4 h (D–F). Images were collected at 2-s intervals; panels shown are 10 s apart. Arrowheads in A indicate microtubules that undergo growing and shortening events. Arrowheads in D indicate stable microtubules. Bar, 2 μm .

the fluorescent tubulin into microtubules, it was necessary to inject the fluorescent tubulin before the addition of taxol to the cells. In addition, previous experiments indicated that intracellular taxol concentrations in HeLa cells attained equilibrium between 1.5 and 6 h after addition of taxol to the cell culture medium (1.5 h for 100 nM taxol and 6 h for 10 nM taxol) (Jordan and Wilson, 1998b). Thus, the following protocol was adopted: after a 90-min incorporation of rhodamine-labeled tubulin into cellular microtubules in the absence of taxol, cells were incubated with taxol for 4 h, and measurements of microtubule behavior were performed in media lacking taxol for 0–2 h after the 4-h taxol incubation. We found that addition of 30 nM taxol to Caov-3 cells for 4 h resulted in an intracellular concentration of $10.7 \pm 0.7 \mu\text{M}$, and addition of 100 nM taxol to A-498 cells for 4 h resulted in an intracellular concentration of $19.6 \pm 2.6 \mu\text{M}$ (Table 1). These data show that the intracellular concentration of taxol reached approximate equilibrium during the 4-h incubation and that the intracellular concentrations in the two cell lines were similar using this regimen.

Figure 2, A–C, shows the lamellar region of a living, untreated Caov-3 cell that was microinjected with rhodamine-labeled tubulin and observed using low light level fluorescence microscopy (see MATERIALS AND METHODS). Consistent with previous results in other cell types (Cassimeris *et al.*, 1988; Sammak and Borisy, 1988; Schulze and Kirschner, 1988; Shelden and Wadsworth, 1993; Dhamodharan *et al.*, 1995), the plus ends

of microtubules alternated between phases of growing, shortening, and a paused state (a state of attenuated dynamic activity). The arrangement and dynamic behavior of rhodamine-labeled microtubules in A-498 cells was similar to that in Caov-3 cells (our unpublished results).

Life history plots show the position of individual microtubule plus ends over time (Figure 3); these graphs were used to determine the parameters of dynamic instability (Tables 2 and 3). Plus ends of microtubules in control Caov-3 cells shortened at $11.5 \pm 7.3 \mu\text{m}/\text{min}$, faster than their mean growing rate of $8.3 \pm 4.5 \mu\text{m}/\text{min}$. Plus ends of microtubules in control A-498 cells shortened and grew at similar rates ($9.2 \pm 5.1 \mu\text{m}/\text{min}$ and $8.4 \pm 4.2 \mu\text{m}/\text{min}$, respectively). As indicated by the large SDs, wide variations in the growing and shortening rates occurred, consistent with previous measurements (Gildersleeve *et al.*, 1992). Interestingly, the values for the parameters of microtubule dynamics in both tumor cell lines were generally lower than the values measured in other cell types (see DISCUSSION).

Low Concentrations of Taxol Strongly Suppress Shortening and Growth Excursions

As shown in the video sequence and life history plots (Figures 2 and 3), incubation of Caov-3 cells with 30 nM taxol markedly suppressed the dynamic behavior of the microtubules. In Figure 2, D–F, the reduction in

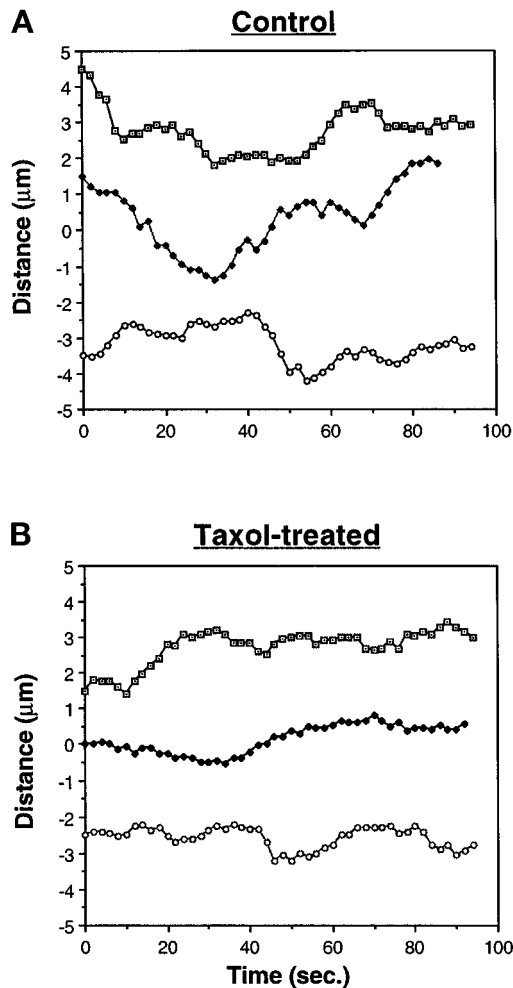


Figure 3. Life history plots of microtubules in control (A) and taxol-treated (B) Caov-3 cells. The graphs represent the excursions made by individual microtubules during an 86- to 94-s observation period. Microtubules in the presence of taxol are characterized by longer pause events and less extensive growing and shortening events than those in control cells. The plots are offset on the *y*-axis for clarity.

dynamic behavior of the microtubules is evident by following the ends of the microtubules marked by the arrowheads. The mean shortening rate was significantly reduced by taxol in both cell lines (95–99% confidence level) (Table 2). The mean shortening rate was reduced by 31% in Caov-3 cells (from $11.6 \pm 7.3 \mu\text{m}/\text{min}$ in controls to $7.9 \pm 7.2 \mu\text{m}/\text{min}$ at 30 nM taxol) and by 26% in A-498 kidney cells (from $9.2 \pm 5.1 \mu\text{m}/\text{min}$ to $6.7 \pm 3.2 \mu\text{m}/\text{min}$ at 100 nM taxol). Taxol also significantly suppressed the average rate of microtubule growth in both cell lines (95–99% confidence level). The rates of growth were suppressed by 24% in ovarian cells (from $8.3 \pm 4.5 \mu\text{m}/\text{min}$ to $6.3 \pm 3.7 \mu\text{m}/\text{min}$ at 30 nM taxol) (Table 2) and by 18% in kidney cells (from $8.4 \pm 4.2 \mu\text{m}/\text{min}$ to 6.8 ± 4.0

$\mu\text{m}/\text{min}$ at 100 nM taxol). In addition, taxol reduced the lengths of shortening and growing events in both cell lines. In Caov-3 cells 30 nM taxol reduced the lengths of shortening and growing by 16% and 21%, respectively (from $1.41 \pm 1.0 \mu\text{m}$ to $1.18 \pm 1.2 \mu\text{m}$, and from $1.23 \pm 1.1 \mu\text{m}$ to $0.97 \pm 0.65 \mu\text{m}$, respectively), and in A-498 cells 100 nM taxol reduced the lengths of shortening and growing by 27% and 34%, respectively (from $0.97 \pm 0.7 \mu\text{m}$ to $0.71 \pm 0.2 \mu\text{m}$, and from $0.87 \pm 0.7 \mu\text{m}$ to $0.57 \pm 0.1 \mu\text{m}$, respectively, significant at 95–99% confidence levels) (Table 3). Thus, taxol strongly decreased the rates and lengths of microtubule shortening and growth in both ovary and kidney tumor cells.

Taxol Increased the Frequency of Rescue

The transition of a microtubule end from shortening to growth or pause is called rescue, and the transition from growth or pause to shortening is called catastrophe (Walker *et al.*, 1988). We examined the frequencies of rescue and catastrophe in two ways: by measuring the distance a microtubule grew or shortened before the transition or by measuring the duration of the phase before the transition. In both cell types, taxol increased the distance-based rescue frequency but had no effect on the time-based rescue frequency (Table 3). The rescue frequency increased in Caov-3 cells by 25% (from $0.60/\mu\text{m}$ in controls to $0.76/\mu\text{m}$ at 30 nM taxol) and in A-498 cells by 58% (from $0.92/\mu\text{m}$ in controls to $1.46/\mu\text{m}$ at 100 nM taxol). Taxol also reduced the time-based frequency of catastrophe in A-498 cells by 58% but had no detectable effect on the time-based catastrophe frequency in Caov-3 cells. This difference between the two cell lines is most likely due to the fact that the percentage of time in pause (which contributes to the denominator of the time-based catastrophe frequency) was increased in A-498 cells at the taxol concentrations used but was not altered significantly in Caov-3 cells (discussed below).

Taxol Increased the Duration and Percentage of Time in the Paused (Attenuated) State in A-498 Cells

Pauses are periods during which growth or shortening at microtubule ends is not detectable. We assume that tubulin addition to and loss from microtubule ends continue at attenuated, but undetectable, rates at microtubule ends during phases of pause or attenuation. In A-498 kidney cells, the average pause duration increased significantly (99.9% confidence level) by 74%, from $12.8 \pm 13.6 \text{ s}$ in controls to $22.3 \pm 18.3 \text{ s}$ in 100 nM taxol. The overall percentage of time in pause also increased, from 60.7% to 79.6%. In contrast, there was not a significant increase in the duration or percentage of time in pause in Caov-3 cells (Table 3). The difference between the two cell lines may result from

Table 2. Effects of taxol on rates of microtubule dynamic instability in human tumor cells

Parameter	Cell type and taxol concentration					
	A-498 control	A-498 + 100 nM	Change	Caov-3 control	Caov-3 + 30 nM	Change
Growth rate ($\mu\text{m}/\text{min}$)	8.36 ± 4.2	6.83 ± 4.0^a	-18%	8.27 ± 4.5	6.30 ± 3.7^b	-24%
Shortening rate ($\mu\text{m}/\text{min}$)	9.15 ± 5.1	6.74 ± 3.2^b	-26%	11.55 ± 7.3	7.91 ± 7.2^a	-32%

The values are expressed as \pm SD.
^a Values significant at 95% confidence level (Student's *t* test).
^b Values significant at 99% confidence level (Student's *t* test).

the inherently slower dynamics of A-498 cell microtubules (their control shortening rate was 21% slower than in Caov-3 cells). Thus taxol-induced suppression of shortening might result in more events in A-498 cells falling into the pause category, where dynamics are undetectable by microscopy, than in Caov-3 cells.

Taxol Reduced Dynamicity in Both Cell Lines

Dynamicity is the summed gain and loss (exchange) of tubulin subunits at the microtubule ends and is a measure of overall dynamic instability. In both cell lines, taxol significantly reduced the dynamicity, by 31% at 30 nM taxol in Caov-3 cells and by 63% at 100 nM taxol in A-498 cells (Table 3).

Effects of Taxol on the Arrangement of Interphase and Mitotic Microtubules

Analysis of the dynamic behavior of individual microtubules in living cells is limited to the peripheral regions of interphase cells; the arrangement and behavior of microtubules in other regions of the cell and during mitosis are not readily recorded by this method. Analysis of individual microtubule dynamic behavior in mitotic cells is difficult given the rounded nature of the cells and the density of microtubules in the spindle and asters. Thus, we used immunofluorescence microscopy of fixed cells to compare the effects of taxol (4-h incubation) on the arrangement of microtubules in interphase cells (Figure 4) with the arrangement of microtubules in mitotic cells (Figure 5).

Table 3. Effects of taxol on parameters of microtubule dynamic instability in living human tumor cells

Parameter	Cell type and taxol concentration			
	A-498 kidney control	A-498 kidney + 100 nM	Caov-3 ovarian control	Caov-3 ovarian + 30 nM
Number of microtubules	40	26	36	34
S-length (μm) ^a	0.97 ± 0.7	0.71 ± 0.2^b	1.41 ± 1.0	1.18 ± 1.2
S-duration (s)	7.43 ± 4.7	7.53 ± 4.5	8.25 ± 4.8	9.62 ± 4.7
G-length (μm) ^a	0.87 ± 0.7	0.57 ± 0.1^c	1.23 ± 1.1	0.97 ± 0.65
G-duration (s)	7.01 ± 4.0	6.35 ± 3.5	9.84 ± 8.1	9.88 ± 4.7
Pause duration (s)	12.78 ± 13.6	22.29 ± 18.3^d	14.5 ± 15.6	16.9 ± 16.5
Pause (% of total time)	60.7	79.6	62.9	66.7
Growth (% of total time)	18.9	10.8	23.9	19.5
Shortening (% of total time)	20.4	9.6	13.2	13.8
Catastrophe frequency (events/s)	0.033	0.014	0.018	0.017
Rescue frequency (events/s)	0.120	0.137	0.103	0.093
Catastrophe frequency (events/ μm)	1.13	1.26	0.506	0.765
Rescue frequency (events/ μm)	0.923	1.46	0.604	0.755
Dynamicity ($\mu\text{m}/\text{min}$)	3.01	1.12	3.13	2.17

The values are expressed as mean or mean \pm SD.

^a S, Shortening; G, growing.

^b Values significant at 95% confidence level (Student's *t* test).

^c Values significant at 99% confidence level (Student's *t* test).

^d Values significant at 99.9% confidence level (Student's *t* test).

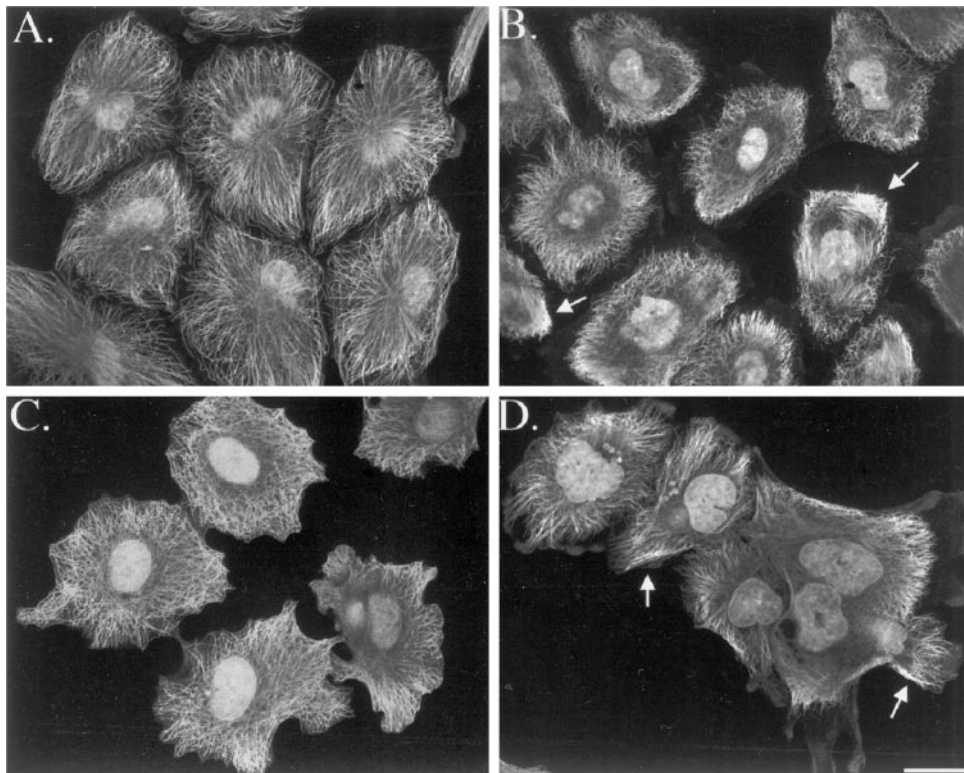


Figure 4. Arrangement of microtubules in A-498 kidney cells (A, B) and Caov-3 ovary cells (C, D) in interphase in the absence (A, C) or presence (B, 100 nM; D, 30 nM) of taxol (4-h incubation). Cells were stained with an antibody to α -tubulin and imaged using confocal microscopy. A single optical section is shown. Microtubules retracted slightly from the plasma membrane and formed occasional bundles (arrows in B and D) after taxol incubation. Bar, 20 μ m.

As shown in Figure 4, A and C, in untreated interphase A-498 and Caov-3 cells, the microtubules were long, relatively straight, and radiated from the cell center toward the periphery, filling the cytoplasm. After incubation of Caov-3 cells in 30 nM taxol and A-498 cells in 100 nM taxol, the microtubules no longer extended to the edges of the cell; rather a peripheral region devoid of microtubules was present in many cells (Figure 4, B and D). In addition, a few bundles of short (~ 10 – 20μ m) microtubules formed (indicated by arrows in Figure 4, B and D). The bundles in Caov-3 cells were thin and radially oriented, whereas the bundles in A-498 cells were thicker and oriented parallel to the cell membrane. Note that cells incubated in taxol were more rounded than control cells, and thus, in confocal optical sections, the perinuclear regions often appeared to lack microtubules because regions of the cell that were farthest from the substrate were excluded from the image. In most cases, the apparent lack of microtubules was due to microtubules leaving the plane of the optical section shown; however, in other cases, the distribution of microtubules near peripheral bundles was nonuniform. The overall mass of microtubules was not altered significantly, as assessed by microscopy, in the two cell lines at these taxol concentrations.

The arrangement of microtubules in mitotic cells was also examined after fixation and staining for mi-

crotochules and chromosomes (Figure 5). Taxol induced significant abnormalities in spindle organization in both cell types. No completely normal spindles remained. Abnormal spindles were generally either bipolar, with "lagging" chromosomes remaining at the spindle poles (Figure 5B), or multipolar, with multiple asters of microtubules and disorganized chromosomes (Figure 5D). In Caov-3 cells (30 nM taxol; Figure 5D), the majority of spindles were multipolar, whereas in A-498 cells (100 nM taxol, Figure 5B), bipolar spindles with many lagging chromosomes were more frequently observed.

Taxol Blocks Mitotic Progression in Caov-3 and A-498 Cells

Interestingly, no anaphase or telophase figures were observed in the fixed and stained preparations, suggesting that taxol blocked progression through mitosis. To quantify this observation, we measured mitotic block and the percentage of cells in mitosis for cells incubated with taxol at the concentrations that inhibited microtubule dynamics and cell proliferation (data represent means and SEs of three to five independent experiments per cell line).

In Caov-3 cells, the proportion of cells in mitosis increased fivefold, from $1.2 \pm 0.2\%$ in controls to $6.1 \pm 0.5\%$ in 30 nM taxol. Not only did taxol slow mitosis,

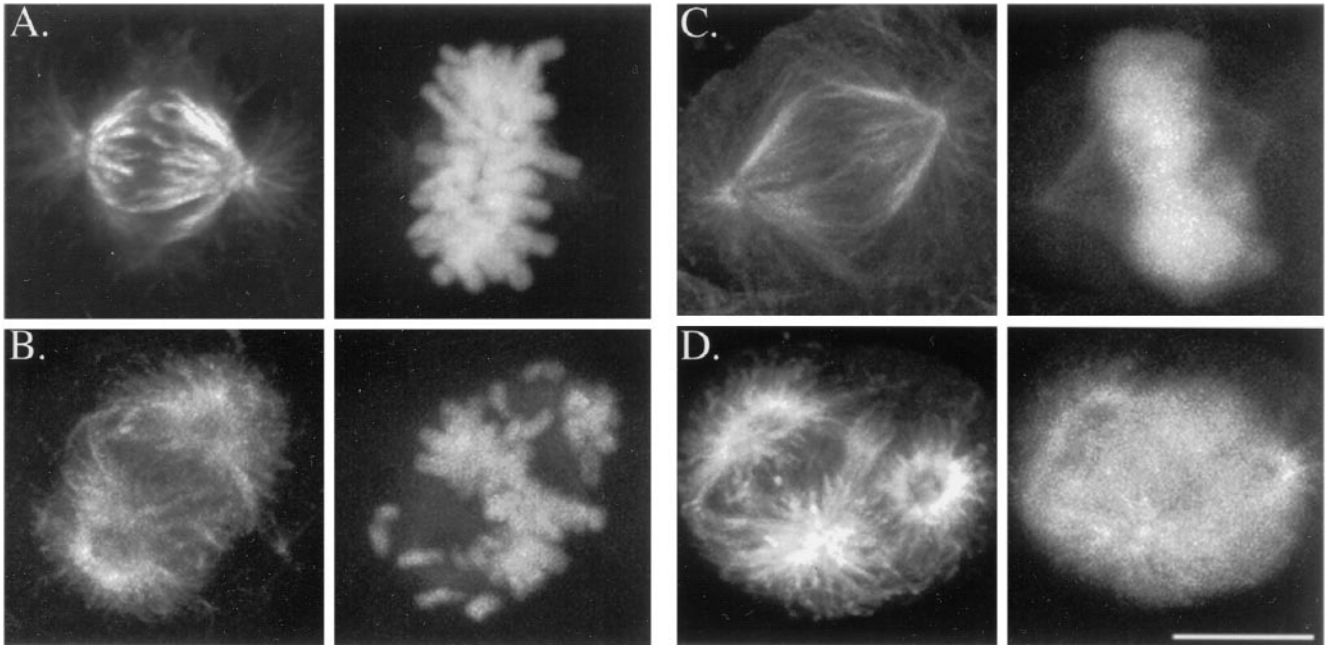


Figure 5. Microtubules in mitotic A-498 kidney cells (A, B) and Caov-3 ovary cells (C, D) in the absence (A, C) or presence (B, D) of taxol (100 nM and 30 nM, respectively). Cells were incubated with taxol and stained for microtubules (left panels) as described for Figure 4. They were subsequently stained with propidium iodide for DNA (right panels of each pair), and an extended focus series using confocal microscopy was collected. (A, B) Control spindles are bipolar, with congressed chromosomes forming a compact metaphase plate midway between the poles. After 4-h incubation with taxol, spindle morphology is dramatically altered. Many spindles are multipolar (D) with uncongressed chromosomes (B and D). Bar, 10 μ m.

but it prevented progression into anaphase and induced significant abnormalities in spindle organization. No Caov-3 cells progressed to anaphase at taxol concentrations ≥ 10 nM, and all mitotic spindles were abnormal in organization. Similarly, in A-498 kidney cells, the proportion of cells in mitosis increased 9.4-fold, from $2.0 \pm 0.1\%$ in controls to $15.1 \pm 2.4\%$ in 100 nM taxol. Also, at taxol concentrations ≥ 100 nM, no A-498 cells progressed from metaphase to anaphase, and all mitotic spindles were abnormal in organization. For example, at 100 nM taxol, $77.8 \pm 2.8\%$ of spindles were multipolar, and the remaining spindles either were bipolar, with chromosomes remaining at the spindle poles, or were monopolar balls of disorganized chromosomes.

Taxol also induced abnormalities in both types of cells in interphase. Cells contained several large or lobulated nuclei or many smaller nuclei (Figure 4). At 100 nM taxol, $70.7 \pm 1.7\%$ of interphase A-498 cells were multinucleate compared with $3.0 \pm 1.1\%$ in controls. At 30 nM taxol, $29.7 \pm 3.4\%$ of interphase Caov-3 cells were multinucleate compared with $1.4 \pm 0.3\%$ in controls (mean and SE of three to five independent experiments per cell line). Together these results suggest that in taxol, cancer cells did not proliferate because they could not complete mitosis and ultimately

reverted to an abnormal multinucleate interphase condition.

During prolonged incubation in 100 nM taxol for 48–72 h, A-498 and Caov-3 cells did not recover and resume proliferation but began to die. The numbers of live and dead cells were counted after incubation in taxol for 72 h by staining of unfixed cultures with calcein AM and ethidium bromide (see MATERIALS AND METHODS). At 30 nM taxol (72 h), $25.4 \pm 2.1\%$ of the remaining Caov-3 cells were dead, as compared with $3.9 \pm 1.1\%$ in controls. At 100 nM taxol (72 h), 16% of the remaining A-498 cells were dead. (Cells that may already have died and lysed would not be detected by this method.) The result of these effects was inhibited proliferation and cell death in both cell lines.

DISCUSSION

We have shown that in living cells of two diverse human tumor lines, concentrations of taxol that blocked cell proliferation significantly suppressed microtubule dynamic instability. At 30–100 nM added taxol, rates and lengths of microtubule shortening and growing were inhibited, the duration of pause events was increased, the percentage of time in pause was

increased, and the overall dynamicity of the microtubules was inhibited. Suppression of dynamic instability was associated with aberrant organization of mitotic spindles and complete inhibition of progress into anaphase. The results suggest that inhibition of microtubule dynamics is the most potent chemotherapeutic mechanism of taxol.

Determination of Microtubule Dynamics in Living Human Tumor Cells

Dynamic instability varies significantly among cells types; for example, microtubule dynamic turnover is significantly greater in mammalian fibroblasts (Chinese hamster ovary) than in epithelial cells (potoroo kidney [PtK1]) (Shelden and Wadsworth, 1993). Previous determinations of microtubule dynamics in living cells have not included human cells. One important question we addressed is whether the dynamics of microtubules in human tumor cells differ significantly from those of other mammalian cell types. For example, cancer cells are characterized by deregulation of the cell cycle and are often more motile and/or less adhesive than normal cells; these changes might be associated with an increase in microtubule dynamics. The parameters of microtubule dynamics have been obtained by similar methods in five types of living mammalian cells: PtK1, monkey kidney (BSC-1), Chinese hamster ovary, and, in this study, A-498 human kidney and Caov-3 human ovary. Interestingly, in the present study we found that dynamic instability of microtubules is significantly lower in A-498 and Caov-3 cells than in other mammalian cell lines. The percentage of time in pause or attenuation was significantly greater in microtubules of human tumor A-498 and Caov-3 cells (60.7% and 62.9%; Table 3) than in either PtK1 cells (38%) or BSC-1 cells (33.4%) (Dhamodharan *et al.*, 1995; Shelden and Wadsworth, 1996). In addition, dynamicity, the overall measure of subunit loss and gain from microtubule ends, was slower in the human tumor cells than in other cell types: 3.0 $\mu\text{m}/\text{min}$ for A-498 and 3.1 $\mu\text{m}/\text{min}$ for Caov-3 (Table 3), compared with 5.6 $\mu\text{m}/\text{min}$ for PtK1 and 7.2 $\mu\text{m}/\text{min}$ for BSC-1 (Dhamodharan and Wadsworth, 1995; Shelden and Wadsworth, 1996). The origin and meaning of these differences is not clear, but they indicate that, contrary to expectations, human tumor cells in interphase have slow microtubule dynamics relative to other cell types.

Similarity of the Effective Taxol Concentrations in Caov-3 and A-498 Cells

The minimum taxol concentration that completely blocked proliferation in Caov-3 cells was 30 nM added to the medium, resulting in an intracellular concentration of $10.7 \pm 0.7 \mu\text{M}$ at 4 h, and $\sim 20 \mu\text{M}$ at 24 h (Table 1). More added taxol (100 nM) was required to com-

pletely block proliferation in A-498 cells; 100 nM taxol added to the medium resulted in an intracellular concentration of $19.6 \pm 2.6 \mu\text{M}$ at 4 h and remained approximately the same at 24 h ($17.4 \pm 1.8 \mu\text{M}$). The higher concentrations of added taxol required to achieve a 17–20 μM intracellular concentration and inhibit proliferation of A-498 kidney cells may be explained, at least in part, by the high levels of multi-drug resistance (MDR-1 gene) mRNA in A-498 cells leading to reduction in uptake or retention of chemotherapeutic drugs (Wu *et al.*, 1992). Interestingly, the intracellular taxol concentrations that effectively suppressed dynamics and progress into anaphase were similar in the two cell lines. Thus, the data from these two cell types provide a very limited negative indication of differential taxol sensitivity of microtubules as a basis for the differential sensitivity of tumor types to taxol. Clearly much more experimentation is necessary to resolve this question.

Qualitative Effects of Taxol on Microtubule Dynamics in Human Tumor Cells Closely Resemble Its Effects on Bovine Brain Microtubules In Vitro

The suppressive effects of taxol on dynamic instability of microtubules in Caov-3 cells and in A-498 cells strongly resemble its effects on dynamic instability of microtubules assembled from purified bovine brain tubulin (Derry *et al.*, 1995). The shortening rate is inhibited strongly both in cells and in vitro, and the rate of growth is also inhibited. For example, 25 nM taxol inhibited the shortening rate of microtubules composed of bovine brain tubulin by 32% and inhibited the growing rate by 20%. Comparable inhibition of shortening and growing rates was observed in cells (24–32% inhibition of shortening rates and 18–26% inhibition of growing rates) at added taxol concentrations of 100 nM for A-498 cells and 30 nM for Caov-3 cells (Table 2); however, as mentioned above, taxol accumulated intracellularly to high concentrations (11–20 μM ; Table 2). Thus the taxol concentrations that inhibited dynamics were 500- to 800-fold higher in cells than in vitro. Similarly, 11–20 μM in cells increased the catastrophe frequency per micrometer by 12–51% and the rescue frequency per micrometer by 25–58%, whereas 25 nM taxol in vitro increased the catastrophe and rescue frequencies per micrometer by 62 and 18%, respectively. Thus, taxol appears significantly less potent in suppressing dynamics of microtubules in living human tumor cells than in bovine brain microtubules reassembled in vitro.

The apparent reduction in potency of taxol in cells has several possible causes. Taxol is poorly soluble in water; thus taxol may be sequestered in lipophilic compartments or cell membranes so that the drug is not entirely available to bind to microtubules. Taxol has been shown to differentially inhibit dynamics of

microtubules of different isotype compositions in vitro (Derry *et al.*, 1997) and to induce synthesis of additional cellular tubulin (Jordan *et al.*, 1993); both phenomena might alter the effects on dynamics in cells. In addition, microtubules in cells may be less sensitive to bound taxol for reasons that we do not currently understand. For example, the dynamics of microtubules in interphase cells (although slow compared with dynamics in mitosis) are approximately threefold faster than those of reassembled bovine brain microtubules in vitro (compare shortening and growing rates of 8–12 $\mu\text{m}/\text{min}$ in cells in interphase with rates of 3–5.4 $\mu\text{m}/\text{min}$ in vitro). The dynamics of microtubules in cells are regulated by endogenous cellular proteins such as stathmin (metablastin or op 18) (Belmont and Mitchison, 1996; Horwitz *et al.*, 1997) and by posttranslational changes in tubulin such as phosphorylation and glutamylation (Ludueno, 1998). These regulatory factors may counteract the effects of taxol in cells by stimulating microtubule turnover. In addition, competition for taxol binding sites by endogenous regulators may occur in vivo.

Kinetic Stabilization of Microtubule Ends by Taxol in Cells Resembles Stabilization by Vinblastine and Nocodazole

Taxol blocks or slows mitosis and inhibits cell proliferation in a manner similar to other antimitotic compounds that alter the assembly dynamics of microtubules (Jordan *et al.*, 1992; Dhamodharan *et al.*, 1995; Vasquez *et al.*, 1997). We previously found that concentrations of vinblastine (32 nM) that slowed mitosis fourfold and inhibited proliferation by 60–70% in monkey kidney cells (BSC-1) resulted in 20% inhibition of the microtubule growing rates, 67% inhibition of the shortening rates, 50% inhibition of the growing lengths, and 71% inhibition of the shortening lengths. These effects took place in the absence of measurable microtubule depolymerization (Dhamodharan *et al.*, 1995). Nocodazole (4–100 nM), a compound that induces mitotic arrest (DeBrabander *et al.*, 1976; Zieve *et al.*, 1980; Jordan *et al.*, 1992), also suppresses the rates and lengths of microtubule excursions in BSC-1 cells and newt lung cells (Vasquez *et al.*, 1997).

Thus the general mechanism of mitotic block by taxol, vinca alkaloids, nocodazole, and many other mitotic poisons such as colchicine, cryptophycins, and dolastatins appears to involve suppression of the dynamics of mitotic spindle microtubules (Jordan and Wilson, 1998). Suppression of microtubule dynamics may arrest mitosis by preventing attachment of spindle microtubules to kinetochores. Low concentrations of vinblastine reduce the number of microtubules attached to kinetochores (Wendell *et al.*, 1993), and reduction in microtubule attachment to kinetochores has been implicated in mitotic arrest by taxol (Waters *et al.*,

1998). Alternatively, by suppressing microtubule dynamics these drugs may reduce tension on kinetochores (Wendell *et al.*, 1993; Rieder *et al.*, 1994; Li and Nicklas, 1995; Rieder *et al.*, 1995), thus triggering the spindle assembly checkpoint and blocking mitosis.

Chemotherapeutic Mechanism of Taxol

The results presented here indicate that the cellular process that is most sensitive to taxol is suppression of microtubule dynamics; i.e., microtubule dynamics are suppressed in the absence of any other detectable alteration in cellular organelles, including the absence of significant bundling of microtubules. In addition, suppression of dynamics occurs at the lowest taxol concentrations that inhibit cell proliferation, and in concert with blockage or slowing of mitosis. These results indicate that the formation of properly organized and functional spindles, which are able to progress through the mitotic checkpoint, is extremely sensitive to inhibition of microtubule dynamics. Previous studies indicate that mitotic block by taxol, even at very low taxol concentrations, leads to apoptosis in human tumor cells (Jordan *et al.*, 1996), possibly through downstream events that may involve phosphorylation of bcl2 (Blagosklonny *et al.*, 1996, 1997; Haldar *et al.*, 1997).

Plasma concentrations of taxol during chemotherapy in cancer patients are consistent with the model that taxol exerts its most potent chemotherapeutic effects by suppressing microtubule dynamics and thus disrupting mitosis. After a 3-h intravenous infusion of taxol, Walle *et al.* (1995) found that taxol concentrations in human plasma decreased at a faster than exponential rate over a 12-h period, ranging from a peak of 8 μM at the termination of the infusion to a low of 80 nM 12 h later. In addition, ~88–97% of plasma taxol is bound to plasma proteins (reviewed in Sparreboom *et al.*, 1998), thus reducing the available taxol concentration in plasma ~10- to 20-fold, to effective concentrations of 4–800 nM. Thus the taxol concentrations used in the experiments reported here (30–100 nM), which significantly suppress microtubule dynamics and block mitosis, fall in the range of effective plasma taxol concentrations in humans during chemotherapy.

Overall, the results indicate that subtle suppression of microtubule dynamics by taxol has dramatic deleterious effects on the ability of a cancer cell to properly assemble a functioning mitotic spindle, to pass the metaphase/anaphase checkpoint, and to produce progeny cells. They also suggest that the most sensitive chemotherapeutic mechanism of taxol is inhibition of cancer cell proliferation by suppression of dynamic instability of mitotic spindle microtubules. These results are corroborated by findings that low nanomolar concentrations of taxol inhibit the dynam-

ics of mitotic spindle microtubules in a taxol concentration-dependent manner in concert with block at the metaphase/anaphase transition in human tumor cells (J. Kelling, M. A. Jordan, L. Wilson, and K. Sullivan, unpublished observations). Interestingly, taxol does not appear to block the disassembly of the interphase microtubule array; we did not observe cells with condensed chromosomes or duplicated poles that retained an interphase microtubule array. Thus the stabilization of microtubules by taxol does not prevent entry into mitosis but is sufficient to block cells in mitosis by disrupting the assembly and function of the mitotic spindle.

ACKNOWLEDGMENTS

We thank Jonathan Kroopnik, Keith DeLuca, and Kim Wendell for analysis of microtubule dynamics and excellent technical assistance, and Vivian Ngan and Leslie Wilson for critical reading of this manuscript. This work was supported by National Institutes of Health grant CA-57291 and National Science Foundation grant MCB-9304646.

REFERENCES

- Belmont, L.D., and Mitchison, T.J. (1996). Identification of a protein that interacts with tubulin dimers and increases the catastrophe rate of microtubules. *Cell* 84, 623–631.
- Blagosklonny, M.V., Giannakakou, P., El-Deiry, W.S., Kingston, D.G.I., Higgs, P.I., Neckers, L., and Fojo, T. (1997). Raf-1/bcl2 phosphorylation: a step from microtubule damage to cell death. *Cancer Res.* 57, 130–135.
- Blagosklonny, M.V., Schulte, T., Nguyen, P., Trepel, J., and Neckers, L. (1996). Taxol-induced apoptosis and phosphorylation of bcl-2 protein involves c-Raf-1 and represents a novel c-Raf-1 signal transduction pathway. *Cancer Res.* 56, 1851–1854.
- Caplow, M., Shanks, J., and Ruhlen, R. (1994). How taxol modulates microtubule disassembly. *Biochemistry* 269, 23399–23402.
- Cassimeris, L., Pryer, N.K., and Salmon, E.D. (1988). Real-time observations of microtubule dynamic instability in living cells. *J. Cell Biol.* 107, 2223–2231.
- DeBrabander, M.J., Van de Veire, R.M.L., Aerts, F.E.M., Borgers, M., and Janssen, P.A.J. (1976). The effects of methyl [5-(2-thienylcarbonyl)-1H-benzimidazol-2-yl]carbamate (R 17934; NSC 238159), a new synthetic antitumoral drug interfering with microtubules, on mammalian cells cultured in vitro. *Cancer Res.* 36, 905–916.
- Derry, W., B., Wilson, L., and Jordan, M.A. (1995). Substoichiometric binding of taxol suppresses microtubule dynamics. *Biochemistry* 34, 2203–2211.
- Derry, W.B., Wilson, L., and Jordan, M.A. (1998). Low potency of taxol at microtubule minus ends: implication for its antimetabolic and therapeutic mechanism. *Cancer Res.* 58, 1177–1184.
- Derry, W.B., Wilson, L., Khan, I.A., Luduena, R.F., and Jordan, M.A. (1997). Taxol differentially modulates the dynamics of microtubules assembled from unfractionated and purified β -tubulin isotypes. *Biochemistry* 36, 3554–3562.
- Dhamodharan, R.I., Jordan, M.A., Thrower, D., Wilson, L., and Wadsworth, P. (1995). Vinblastine suppresses dynamics of individual microtubules in living cells. *Mol. Biol. Cell* 6, 1215–1229.
- Dhamodharan, R.I., and Wadsworth, P. (1995). Modulation of microtubule dynamic instability in vivo by brain microtubule associated proteins. *J. Cell Sci.* 108, 1679–1689.
- Diaz, J.F., and Andreu, J.M. (1993). Assembly of purified GDP-tubulin into microtubules induced by taxol and taxotere: reversibility, ligand stoichiometry, and competition. *Biochemistry* 32, 2747–2755.
- Gildersleeve, R.F., Cross, A.R., Cullen, K.E., Fagan, L.P., and Williams, R.C., Jr. (1992). Microtubules grow and shorten at intrinsically variable rates. *J. Biol. Chem.* 267, 7995–8006.
- Haldar, S., Basu, A., and Croce, C.M. (1997). Bcl2 is the guardian of microtubule integrity. *Cancer Res.* 57, 229–233.
- Hayden, J.J., Bowser, S.S., and Rieder, C. (1990). Kinetochore capture astral microtubules during chromosome attachment to the mitotic spindle: direct visualization in live newt cells. *J. Cell Biol.* 111, 1039–1045.
- Horwitz, S., Shen, H., He, L., Dittmar, P., Neef, R., Chen, J., and Schubart, U. (1997). The microtubule-destabilizing activity of metablastin (p19) is controlled by phosphorylation. *J. Biol. Chem.* 272, 8129–8132.
- Horwitz, S.B. (1992). Mechanism of action of taxol. *Trends Pharmacol. Sci.* 13, 134–136.
- Howard, W.D., and Timasheff, S.N. (1988). Linkages between the effects of taxol, colchicine, and GTP on tubulin polymerization. *J. Biol. Chem.* 263, 1342–1346.
- Jordan, M.A., Thrower, D., and Wilson, L. (1992). Effects of vinblastine, podophyllotoxin and nocodazole on mitotic spindles. Implications for the role of microtubule dynamics in mitosis. *J. Cell Sci.* 102, 401–416.
- Jordan, M.A., Toso, R.J., Thrower, D., and Wilson, L. (1993). Mechanism of mitotic block and inhibition of cell proliferation by taxol at low concentrations. *Proc Natl Acad Sci USA* 90, 9552–9556.
- Jordan, M.A., Wendell, K.L., Gardiner, S., Derry, W.B., Copp, H., and Wilson, L. (1996). Mitotic block induced in HeLa cells by low concentrations of paclitaxel (Taxol) results in abnormal mitotic exit and apoptotic cell death. *Cancer Res.* 56, 816–825.
- Jordan, M.A., and Wilson, L. (1998a). Microtubules and actin filaments: dynamic targets for cancer chemotherapy. *Curr. Opin. Cell Biol.* 10, 123–130.
- Jordan, M.A., and Wilson, L. (1998b). The use and action of drugs in analyzing mitosis. In: *Methods in Cell Biology*, vol. 61, Mitosis and Meiosis, ed. C.L. Rieder, San Diego: Academic Press, 267–295.
- Kumar, N. (1981). Taxol-induced polymerization of purified tubulin. *J. Biol. Chem.* 256, 10435–10441.
- Li, X., and Nicklas, R.B. (1995). Mitotic forces control a cell-cycle checkpoint. *Nature* 373, 630–632.
- Luduena, R.F. (1998). Multiple forms of tubulin: different gene products and covalent modifications. *Int. Rev. Cytol.* 178, 207–275.
- Margolis, R.L., and Wilson, L. (1978). Opposite end assembly and disassembly of microtubules at steady state in vitro. *Cell* 13, 1–8.
- McEwen, B., Heagle, A., Cassels, G., Buttle, K., and Rieder, C. (1997). Kinetochore fiber maturation in PK1 cells and its implications for the mechanisms of chromosome congression and anaphase onset. *J. Cell Biol.* 137, 1567–1580.
- Milas, L., Hunter, N.R., Kurdoglu, B., Mason, K.A., Meyn, R., Stephens, L.C., and Peters, L.J. (1995). Kinetics of mitotic arrest and apoptosis in murine mammary and ovarian tumors treated with taxol. *Cancer Chemother. Pharmacol.* 35, 297–303.
- Mitchison, T.J. (1989). Poleward microtubule flux in the mitotic spindle; evidence from photoactivation of fluorescence. *J. Cell Biol.* 109, 637–652.

- Mitchison, T.J., and Kirschner, M. (1984). Dynamic instability of microtubule growth. *Nature* 312, 237–242.
- Panda, D., DeLuca, K., Williams, D., Jordan, M.A., and Wilson, L. (1998). Antiproliferative mechanism of action of cryptophycin-52: kinetic stabilization of microtubule dynamics by high affinity binding of microtubule ends. *Proc. Natl. Acad. Sci. USA* 95, 9313–9318.
- Parness, J., and Horwitz, S.B. (1981). Taxol binds to polymerized tubulin in vitro. *J. Cell Biol.* 91, 479–487.
- Pepperkok, R., Bre, M.H., Davoust, J., and Kreis, T.E. (1990). Microtubules are stabilized in confluent epithelial cells but not in fibroblasts. *J. Cell Biol.* 111, 3003–3012.
- Rieder, C., Schultz, A., Cole, R., and Sluder, G. (1994). Anaphase onset in vertebrate somatic cells is controlled by a checkpoint that monitors sister kinetochore attachment to the spindle. *J. Cell Biol.* 127, 1301–1310.
- Rieder, C.L., Cole, R.W., Khodjakov, A., and Sluder, G. (1995). The checkpoint delaying anaphase in response to chromosome monoorientation is mediated by an inhibitory signal produced by unattached kinetochores. *J. Cell Biol.* 130, 941–948.
- Rodionov, V.I., and Borisy, G.G. (1997). Microtubule treadmilling in vivo. *Science* 275, 215–218.
- Rose, G.G., Pomerat, C.M., Shindler, T., and Trunnell, J. (1958). A cellophane strip technique for culturing tissue in multipurpose culture chambers. *J. Biophys. Biochem. Cytol.* 4, 761–764.
- Rowinsky, E. (1997). The development and clinical utility of the taxane class of antimicrotubule chemotherapy agents. *Annu. Rev. Med.* 48, 353–374.
- Rowinsky, E.K., and Donehower, R.C. (1995). Paclitaxel (Taxol). *N. Engl. J. Med.* 332, 1004–1014.
- Rowinsky, E.K., Donehower, R.C., Jones, R.J., and Tucker, R.W. (1988). Microtubule changes and cytotoxicity in leukemic cell lines treated with taxol. *Cancer Res.* 49, 4093–4100.
- Sammak, P.J., and Borisy, G.G. (1988). Detection of single fluorescent microtubules and methods for determining their dynamics in living cells. *Cell Motil. Cytoskeleton* 10, 237–245.
- Saxton, W.M., Stemple, D.L., Leslie, R.J., Salmon, E.D., Zavortnik, M., and McIntosh, J.R. (1984). Tubulin dynamics in cultured mammalian cells. *J. Cell Biol.* 99, 2175–2186.
- Schiff, P.B., Fant, J., and Horwitz, S.B. (1979). Promotion of microtubule assembly in vitro by taxol. *Nature* 277, 665–667.
- Schiff, P.B., and Horwitz, S.B. (1980). Taxol stabilizes microtubules in mouse fibroblast cells. *Proc. Natl. Acad. Sci. USA* 77, 1561–1565.
- Schulze, E., and Kirschner, M. (1988). New features of microtubule behavior observed in vivo. *Nature* 334, 356–359.
- Shelden, E., and Wadsworth, P. (1993). Observation and quantification of individual microtubule behavior in vivo: microtubule dynamics are cell-type specific. *J. Cell Biol.* 120, 935–945.
- Shelden, E., and Wadsworth, P. (1996). Stimulation of microtubule dynamic turnover in living cells treated with okadaic acid. *Cell Motil. Cytoskeleton* 35, 24–34.
- Sorger, P.K., Dobles, M., Tournebize, R., and Hyman, A.A. (1997). Coupling cell division and cell death to microtubule dynamics. *Curr. Opin. Cell Biol.* 9, 807–814.
- Sparreboom, A., van Tellingen, O., Nooijen, W.J., and Beijnen, J.H. (1998). Preclinical pharmacokinetics of paclitaxel and docetaxel. *Anticancer Drugs* 9, 1–17.
- Vasquez, R.J., Howell, B., Yvon, A.-M.C., Wadsworth, P., and Cassimeris, L. (1997). Nanomolar concentrations of nocodazole alter microtubule dynamic instability in vivo and in vitro. *Mol. Biol. Cell* 8, 973–985.
- Walker, R.A., O'Brien, E.T., Pryer, N.K., Soboeiro, M.F., Voter, W.A., Erickson, H., and Salmon, E.D. (1988). Dynamic instability of individual microtubules analyzed by video light microscopy: rate constants and transition frequencies. *J. Cell Biol.* 107, 1437–1448.
- Walle, T., Walle, U.K., Kumar, G.N., and Bhalla, K.N. (1995). Taxol metabolism and disposition in cancer patients. *Drug Metab. Dispos.* 23, 506–512.
- Waterman-Storer, C., and Salmon, E.D. (1997). Microtubule dynamics: treadmilling comes around again. *Curr. Biol.* 7, 369–372.
- Waters, J.C., Chen, R.H., Murray, A.W., Salmon, E.D. (1998). Localization of Mad2 to kinetochores depends on microtubule attachment, not tension. *J. Cell Biol.* 141, 1181–1191.
- Wendell, K.L., Wilson, L., and Jordan, M.A. (1993). Mitotic block in HeLa cells by vinblastine: ultrastructural changes in kinetochore-microtubule attachment and in centrosomes. *J. Cell Sci.* 104, 261–274.
- Wilson, L., and Jordan, M.A. (1995). Microtubule dynamics: taking aim at a moving target. *Chem. Biol.* 2, 569–573.
- Wu, L., *et al.* (1992). Multidrug-resistant phenotype of disease-oriented panels of human tumor cell lines used for anticancer drug screening. *Cancer Res.* 52, 3029–3034.
- Yvon, A.M., and Wadsworth, P. (1997). Noncentrosomal microtubule formation and measurement of minus end microtubule dynamics in A498 cells. *J. Cell Sci.* 110, 2391–2401.
- Zhai, Y., Kronebusch, P.J., Simon, P.M., and Borisy, G.G. (1996). Microtubule dynamics at the G2/M transition: abrupt breakdown of cytoplasmic microtubules at nuclear envelope breakdown and implications for spindle morphogenesis. *J. Cell Biol.* 135, 201–214.
- Zieve, G.W., Turnbull, D., Mullins, J.M., and McIntosh, J.R. (1980). Production of large numbers of mitotic mammalian cells by use of the reversible microtubule inhibitor nocodazole. *Exp. Cell Res.* 126, 397–405.